8th IEEE International Conference on Automation Science and Engineering
August 20-24, 2012, Seoul, Korea

Weld Seam Detection using Computer Vision for Robotic Arc Welding

Mitchell Dinham and Gu Fang, *Member, IEEE*

Abstract— **Visual identification of narrow welding seams is difficult to achieve in robotic systems especially for ferrous materials. This paper describes an algorithm for detecting the weld seam in a butt-joint configuration for robotic Arc Welding of mild steel materials using computer vision. The proposed method can automatically subtract the background from the images obtained from a robot mounted camera system. Reliable seam identification can then be achieved for welding of ferrous materials. Experimental results have shown that this method is capable of detecting both straight and curved welding seams without prior knowledge of the location of the seam. It is shown that this method is robust to be used in an industrial setting.**

I. Introduction

Currently, robotic welding requires human operators to identify the weld seams and then program the robot to weld them. It can take a significant amount of time and cost to program the robot to weld new parts. This can be justified in a mass production environment as the volume outweighs the initial costs of setting up. However for medium to low volume applications the time and cost of constantly programming a robot for each new production run reduces the benefits so it is more efficient to weld them manually.

To make the process of programming new parts more efficient, computer vision and offline programming techniques have been introduced. In industry, vision systems such as the Fanuc's iR vision [1] have been used to identify pre-taught weld seams and then "shift" the pre-programmed path to accommodate any offsets. Offline simulation programs such as the Fanuc's WeldPro [2] and ABB's robot studio [3] can reduce setup time, however they still require significant human operator interaction and the programs taught in a virtual world will inevitably need to be "touched-up" when applied in the real world due to physical differences between the CAD model and the actual system layout.

To make robotic welding truly flexible the robotic system must be able to automatically identify the weld seam and plan a path to weld it. Computer vision could be used to achieve this. However this presents its own set of challenges as weld assemblies, known as "weldments", generally have very low contrast. Furthermore reflections off shiny metallic surfaces and imperfections such as scratches and millscale can make it difficult for a computer vision system to automatically identify weld seams.

In [4, 5, 6] median filters and smoothing techniques are used along with a binary conversion threshold to segment the image leaving only the weld seam visible. However in these publications the segmentation of the weldment and the background is made easier by the fact that the weldment is made of aluminium which is much highly contrasted against the dark background. The detection is further aided by the fact that the weld seam itself is highly contrasted. The use of "V shaped" chamfers on the edge of the two work pieces aids further in increasing the contrast. In practice however, not all weld seams are prepared in this manner. In the contrary, most square edges are simply pressed against each other for welding. The detection of seams in this type of setting for mild steel plates is more challenging, as it does not present as sharp a contrast as aluminium or stainless steel in a dark background.

Some seam detection algorithms use pre-defined regions of interest (ROI). These are introduced to help focus on the weld seam and ignore background objects. In [7] a pre-defined ROI is located in the centre of the image. The pixel intensities in the local window are used to define a threshold for segmenting the weldment from the background. Similarly in [8] the ROI is centred in the image to ignore background objects. The experimental results show that these methods perform well, however it is not always possible to centre the weld seam in the image for robotic applications due to occlusions introduced from tooling and space limitations.

Leading laser sensor suppliers such as ServoRobot [9] can provide lasers for online detection and tracking of weld seams. However these systems are typically very expensive. In [10] a stereo vision system is used with a laser stripe emitter. The laser is used to emit a single stripe of light across the weld seam, the seam is detected by using the vision system to calculate the point where the light beam changes angle. The use of lasers on seam detection has proven results however they can only be used from a local search perspective and cannot provide global information about the location of weld seams. Therefore lasers are suited to online seam detection and tracking, while not suited for obtaining the overall location of the seam and surrounding obstacles for offline path planning.

The main contribution of this paper is the development of a vision based seam detection algorithm that is capable of automatically detecting narrow weld seams in a butt-joint

Mitchell Dinham is with the School of Computing, Engineering and Mathematics, University of Western Sydney, Australia (e-mail: 15234937@scholar.uws.edu.au).

Gu Fang is with the School of Computing, Engineering and Mathematics, University of Western Sydney, Australia (e-mail: g.fang@uws.edu.au).

configuration. The algorithm is capable of subtracting the background from the image without the use of a pre-defined ROI, leading to the reliable detection of weld seams for ferrous materials such as mild steel.

The proposed algorithm uses the Hough Transform to detect the outside boundary of the weldment so that the background can be removed. Once the background is removed a set of algorithms are used to identify the welding seams. The experiment results show that this method is robust to be used in a workshop environment.

This paper is organized as follows: Section II details the methodology used in the seam detection algorithm. The experimental results are given in Section III followed by the conclusions in Section IV.

I. METHODOLOGY

A. *Overview*

A flowchart describing the overall seam detection process is shown in Fig. 1. In this process, the captured colour images are first set through a 'Pre-processing'. During the pre-processing, the image is first converted to a grayscale image and then is filtered. After this pre-processing, a Background Subtraction method is introduced. This method uses the edge information obtained from the image to search for differences between the background and the foreground. Once the differences are identified, the background can then be removed from the image. Once the background is removed the Seam Detection can then be carried out. In the following sections the details of each stage are given.

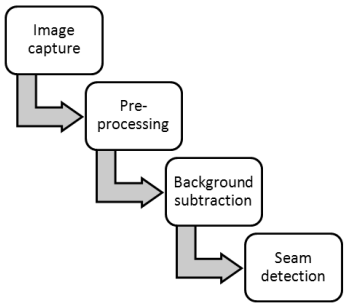

Figure 1. Process flowchart

B. *Pre-processing*

B.1 Image conversion

The first stage in the segmentation of the weldment and the background is to convert the colour image I_{rgb} to a grayscale image I_{gray}. This can be achieved using equation (1).

$$I_{gray}(u,v) = [0.3 \quad 0.59 \quad 0.11] \begin{bmatrix} I_{rgb}\{R\}(u,v) \\ I_{rgb}\{G\}(u,v) \\ I_{rgb}\{B\}(u,v) \end{bmatrix} \qquad (1)$$

Where (u,v) is the pixel co-ordinate, $I_{rgb}\{R\}$, $I_{rgb}\{G\}$, $I_{rgb}\{B\}$ are the red, green and blue components of the RGB image respectively. It is found that by capturing the image in RGB format rather than a single coloured image more information can be retained for better subsequent image processing.

B.2 Median Filter

A Median filter is used to smooth the background so the edge lines associated with scratches and features in the background are reduced when the edge detection is applied.

When a median filter is applied multiple times, the noise/scratches in the image can be reduced further. In this paper it is found that by applying the median filter twice, the resulting image is smooth enough for further processing. The neighbourhood size also affects the filtering results. The effect of using a median filter to smooth the background is shown in Fig. 2. For the images used in this paper, it was found that a neighbourhood size of 10x10 was ideal for this particular background.

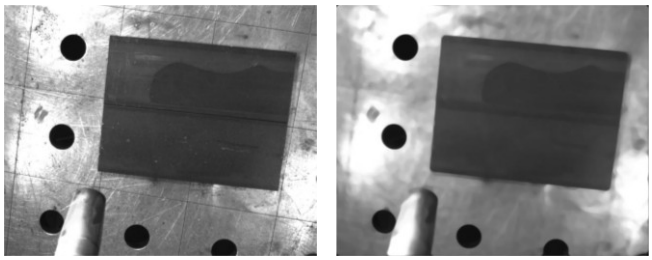

Figure 2. Grayscale image (left) and the image after median filtering (right)

B.3 Edge Detection – Stage 1

In order to use the Hough Transform to detect the outside boundary of the weldment, the edges must first be defined. In this paper, the Sobel edge detection algorithm is used.

The grayscale edge image I_e is then converted to a black and white binary image using an adaptive threshold method [11]. To ensure that the edges of the weldment are unbroken and are clearly defined lines, the binary image undergoes dilation followed by erosion so that the lines have a width of one pixel. The resulting edge image is shown in Fig. 3.

By reducing the edge lines to single pixel width leads to more reliable Houghlines as the groupings in the accumulator are closely matched. This results in a single Houghlines per edge instead of multiple lines therefore reducing the search area.

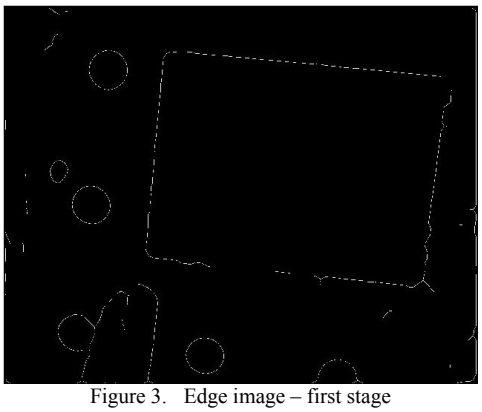

Figure 3. Edge image – first stage

B.4 Hough Transform

Hough transforms can be used to detect straight lines in binary images. Here, Hough lines will be used as a path for the sliding search windows to follow. Houghlines can be described by

$$\rho = u\cos\theta + v\sin\theta \qquad \theta \in) \qquad 2\pi \qquad (2)$$

Where ρ is the distance between the edge point and the image origin and θ is the angle between ρ and the x axis of the image plane. To determine which edge pixels form a straight line, ρ and θ are grouped into bins in an array called the accumulator. Each bin contains a straight line. The highest values in the accumulator are the most defined straight lines in the image [12]. So to limit the number of lines detected a threshold can be placed on the accumulator so that only the strongest edges are returned.

$$T_1 = \beta I_{\max} \qquad (3)$$

Where T_1 is the threshold, β is the threshold multiplier which represents the percentage of the maximum accumulator value H_{max} that will be used. The larger the values of β, the fewer lines are detected. The detected Houghlines (in red) are shown in Fig. 4.

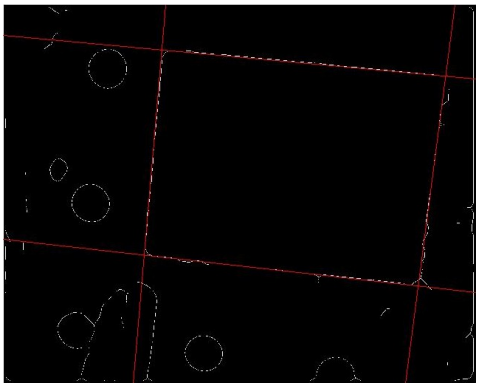

Figure 4. Houghlines, □=0.3

C. Background Subtraction

Currently, existing methods for subtracting the background use a predefined ROI. In this paper, a method of automatically subtracting the background is introduced. This is accomplished by using Houghlines to detect possible edges of the weldment and then using search windows to determine which of those edges belong to the weldment.

The Houghlines in Fig. 4 are broken up into line segments according to the point at which they interest with each other as shown in Fig. 5.

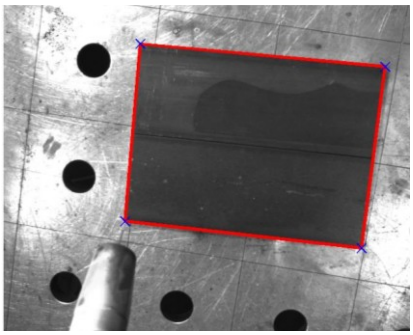

Figure 5. Houghline segments

Each line segment is then used as a path for a set of sliding windows f and g to follow (Fig. 6). The windows are used to compare the value of the grayscale pixel intensity on either side of the line according to the following equations.

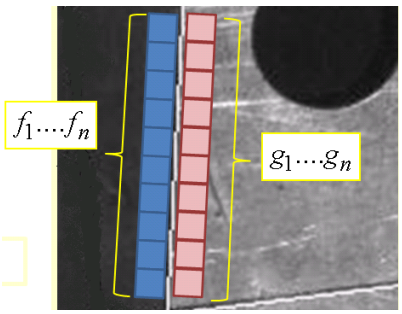

Figure 6. Search windows

$$f_{avg_n} = \sum_{i=}^{w}\sum_{w j=}^{w} I_g(x_n - \frac{w}{2} - 1 + i, y_n - \frac{w}{2} - 1 + j)/(2w) \quad (4)$$

$$g_{avg_n} = \sum_{i=}^{w}\sum_{w j=}^{w} I_g(x_n + \frac{w}{2} + 1 + i, y_n + \frac{w}{2} + 1 + j)/(2w) \quad (5)$$

Where x_n any y_n are the co-ordinates of a point on the line segment, w is the window size and f_{avg_n} and g_{avg_n} are the averaged pixel intensity value in the f_n and g_n windows respectively.

The averaged value of each window is then normalised as a percentage of 255, which is the highest pixel intensity value in a grayscale image and represents the colour white. This gives a base line to measure the difference between the two windows.

$$f_{norm\,n} = \left(\frac{f_{avg\,n}}{255} \right) 00\% \quad (6)$$

$$g_{norm\,n} = \left(\frac{g_{avg\,n}}{255} \right) 00\% \quad (7)$$

Finally, the average value of the normalised windows over the length of the line segment is calculated and the difference compared.

$$F = \frac{\sum_{n=1}^{N} rm_n}{N} \quad (8)$$

$$G = \frac{\sum_{n=1}^{N} rm_n}{N} \quad (9)$$

$$D = |F - G| \quad (10)$$

Where N is the total number of windows on each side of the line segment. The line segment is then on the edge of the weldment and the background if D is greater than a set threshold T_2.

$$Edgeline = \begin{cases} True & D > T_2 \\ False & \end{cases} \quad (11)$$

D is a measure of the average percentage difference between the pixel intensity between the background and weldment. Comparing the edges as the average percentage difference allows for varying lighting conditions such as shadows and bright spots. For example, if the line is along an edge in the background then the value of D will be minimal as the average pixel intensity on either side of the line are similar. If the line is on an edge between the weldment and the background, then depending on the contrast between the two, D will either be small or large but will always be larger than that for the background lines. The threshold as which an edge line is identified correctly is set by T_2. The threshold needs to be a value that is large enough so that false lines are not detected and that the edges of interest are not ignored. It was found that in this paper a value of T_2=10 was sufficient.

Once all the lines have been searched and the boundary lines are returned, the background can be removed by setting all pixels outside the boundary to zero. The resulting image is shown in Fig. 7.

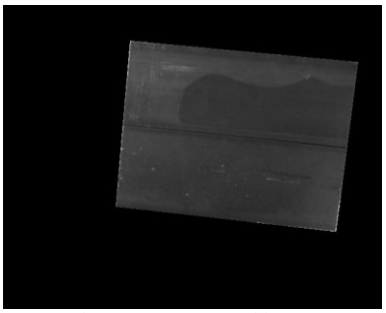

Figure 7. Segmented image

D. Seam Detection

D.1 Edge detection – Stage 2

Once the background has been removed, it is much easier to find the seam line as the search region has been significantly reduced. The Sobel edge detection algorithm is again used to calculate the edge image after using a 3x3 median filter. The median filter is used to smooth image to remove any imperfections such as scratches on the surface of the steel that may show up in the edge image. Using a median filter with a 3x3 neighbourhood was found to reduce the edges from scratches while preserving the edges associated with the seam line. A large neighbourhood will smooth the edges too much resulting in some of the edges not being detected. The resulting edge image is shown in Fig. 8.

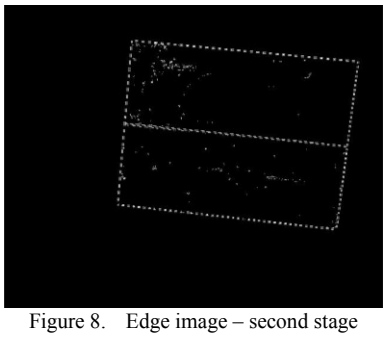

Figure 8. Edge image – second stage

D.2 Boundary Removal

As can be seen by Fig. 8 the seam is clearly visible however there are still a few remaining lines and small clusters of pixels to remove before the seam can be detected. The outside boundary can be removed by calculating the boundary of all 8-connected pixel neighbourhoods. The boundary with the largest value is assumed to be the outside boundary and the pixels associated are set to zero.

The Boundaries can be found by using a contour tracing algorithm such as Moore Neighbourhoods [13]. The pixels comprising the outside boundary are set to zero and is shown in Fig. 9.

D.3 Highlighting the Weld Seam

The remaining small clusters of pixels can be removed by calculating their area and comparing it to a set threshold. If the area is less than the threshold, the pixel values in the cluster can be set to zero according to (12) and therefore be

ignored from seam detection. The resulting image is shown in Fig. 10.

$$I = \begin{cases} 1 & Area > T_3 \\ 0 & \end{cases} \quad (12)$$

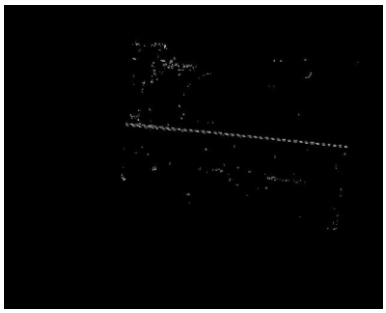

Figure 9. Outside boundary removed

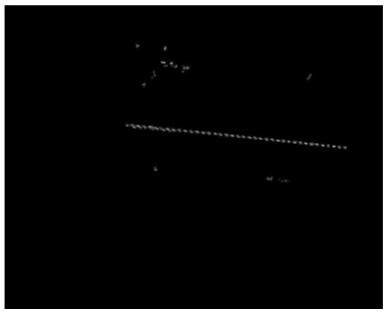

Figure 10. Image after small area removal

In Fig. 10, the seam line can now be clearly seen, with the exception of a few remaining clusters of pixels. To remove these clusters of pixels, the image is dilated and thinned once more to ensure that all pixels on the seam line are connected. The seam line is then found by calculating the length of the remaining pixel clusters along the vertical and horizontal axes of the image plane. The cluster with the longest length in both axes can safely be assumed to be the seam line and is shown in Fig. 11

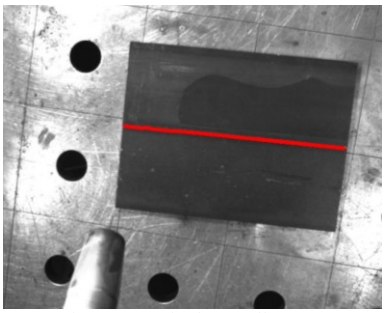

Figure 11. Final seam line

D.4 Post Processing A Algorithm*

To ensure that the seam line is smooth and properly follows contour of the seam, the A* algorithm [14] is used. The A* algorithm is a path planning technique used to find the most efficient path between a starting point and an end point. In terms of post processing the welding seam, it can be used to smooth the line and remove any "spurs" as shown in Fig. 11 and 12. The cost function was set as the Euclidean distance from one pixel to another.

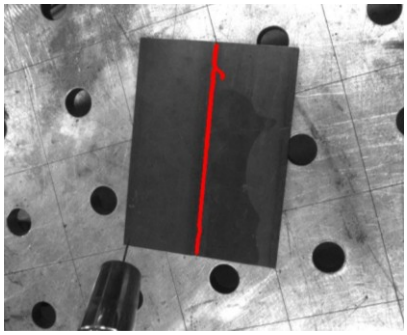

Figure 12. Weld seam before A* post processing

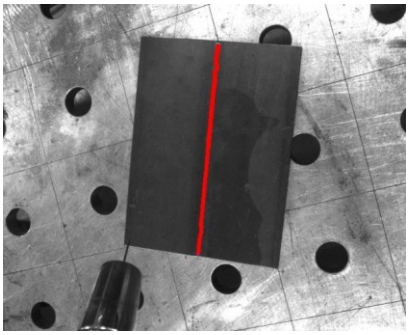

Figure 13. Weld seam after A* post processing

II. RESULTS

The experiments were conducted using a vision system mounted to a welding torch on a Fanuc ArcMate 100iC industrial welding robot. The vision system consisted of two off the shelf USB, 1280×1024 color, *u*Eye CCD cameras as shown in Fig. 13. The weldments are placed on the table and the robot is manually positioned to capture the images.

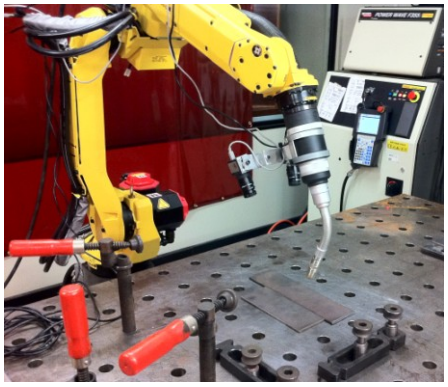

Figure 13. Experiment setup

The seam detection results for various shaped seams are given in Fig. 14, 15, 16 and 17. It can be seen that the seam detection algorithm is capable of not only detecting straight line weld seams but can be used for curved, saw tooth and other various shapes of weld seams. During the experiments the thresholds in equations (3), (4), (5), (11) and (12) were set as follows β=0.3, w=14x14, T_2=10 and T_3=15 respectively. These values hold for all images in this experiment.

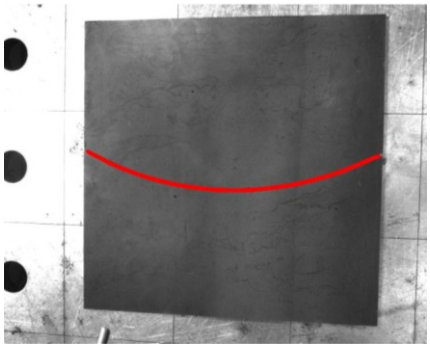

Figure 14. Experiment results for a curved seam

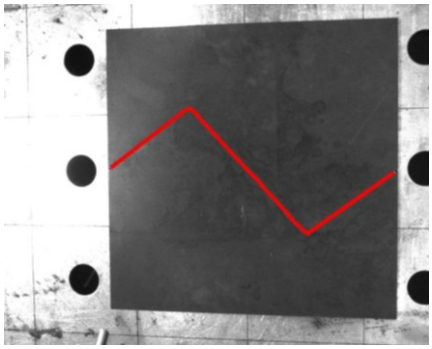

Figure 15. Experiment results for a saw tooth seam

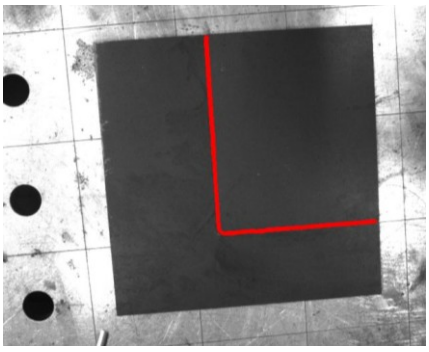

Figure 16. Experiment results for an L-shaped seam

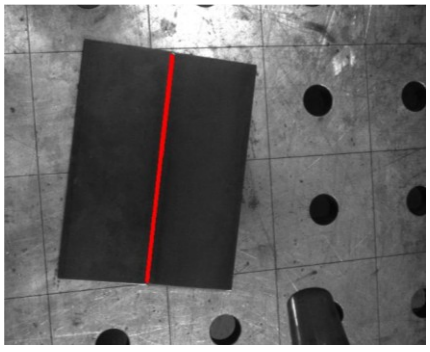

Figure 17. Experiment results for a straight seam

III. CONCLUSION

It can be seen from the experimental results, the proposed seam detection algorithm is capable of detecting weld seams of various shapes and sizes. One of the main advantages of this method is that the seam can be detected without piror knowledge of geometry or location of the seam. It also works well even in the presence of imperfections on the surface of the steel such as scratches and mill scale.

ACKNOWLEDGMENT

This work is supported by the Australian Research Council under project ID LP0991108 and the Lincoln Electric Company Australia.

REFERENCES

[1] Fanuc Robotics, "iR Vision", Fanuc Robotics North America(web), 2012, http://www.fanucrobotics.com/products/vision-software/robot-vision-software.aspx

[2] Fanuc Robotics ,"RoboGuide WeldPro", Fanuc Robotics North America(web),2012, http://www.fanucrobotics.com/products/vision-software/ROBOGUIDE-simulation-software.aspx

[3] ABB , "RobotStudio Software" ABB(web), 2012, http://www.abb.com/product/seitp327/78fb236cae7e605dc1256f1e002a892c.aspx

[4] Kong, M. *et al* "Recognition of the Initial Position of Weld Based on the Corner Detection for Welding Robot in Global Environment" in *Robotic Welding Intelligence & Automation*, LNCIS, (Eds. T.J. Tarn et al), Springer Verlag Berlin Heidelberg, 2007, 362, pp. 249-255.

[5] Micallef, K., Fang, G., Dinham, M., "Automatic Seam Detection and Path Planning in Robotic Welding" in *Robotic Welding Intelligence & Automation*, LNEE, (Eds. T.J. Tarn et al), Springer Verlag Berlin Heidelberg, 2011, 88, pp. 23-32

[6] Pachidis, T.P.,Lygouras, J.N., "Vision-Based Path Generation Method for a Robot Based Arc Welding System" in *Journal of Intelligent Robot Systems*, 2007, 48(3), pp. 307-331.

[7] Dinham, M. Fang, G., Zou, J.J., "Experiments on Automatic Seam Detection for a MIG Welding Robot" in *Artificial Intelligence and Computational Intelligence*, (Eds. H Deng, et al), LNAI 7003, 2011 Springer Verlag Berlin Heidelberg, 2011 pp. 390-397.

[8] Ryberg, A. *et al* , "Stereo Vision for Path Correction in Off-line Programmed Robot Welding" in *Proceedings of the 2010 IEEE International Conference on Industrial Technology*, 2010, pp. 1700-1705.

[9] ServoRobot, "Seam Finding, Seam Tracking and Adaptive Control"ServoRobot(web),2012,http://www.servorobot.com/en/manufacturing-solutions/seam-finding-tracking-adaptive-control.html

[10] He-xi, L., *et al,* "Automatic Teaching of Welding Robot for 3-Dimensional Seam Based on Ant Colony Optimization Algorithm" in *Proceedings of the Second IEEE International Conference on Intelligent Computation Technology and Automation*, 2009, pp. 398-402.

[11] Otsu, N.A., "A Threshold Selection Based on Gray-Level Histograms" in *IEEE Transactions on Systems, Man and Cybernetics*, 1979, 9(1), pp. 62-66.

[12] Shapiro, L., Stockman, G. "Computer Vision", 2001, Prentice Hall

[13] Pavlidis, T. "Algorithms for Graphics and Image Processing", 1982, Computer Science Press, Maryland.

[14] Fang, G., Dissanayake, G., Lau, H., "A Behaviour Based Optimisation Strategy for Multi-Robot Exploration" in *Proceedings of the IEEE International Conference on Robotics, Automation and Robotics*, 2004, pp. 875-879.